

A review of zinc oxide photoanode films for dye-sensitized solar cells based on zinc oxide nanostructures

M.D. Tyona^{*1}, R.U. Osuji^{2a} and F.I. Ezema^{2b}

¹Department of Physics, Benue State University, Makurdi, Nigeria

²Department of Physics and Astronomy, University of Nigeria, Nsukka, Nigeria

(Received August 4, 2012, Revised April 2, 2013, Accepted April 3, 2013)

Abstract. Zinc oxide (ZnO) is a unique semiconductor material that exhibits numerous useful properties for dye-sensitized solar cells (DSSCs) and other applications. Various thin-film growth techniques have been used to produce nanowires, nanorods, nanotubes, nanotips, nanosheets, nanobelts and terapods of ZnO. These unique nanostructures unambiguously demonstrate that ZnO probably has the richest family of nanostructures among all materials, both in structures and in properties. The nanostructures could have novel applications in solar cells, optoelectronics, sensors, transducers and biomedical sciences. This article reviews the various nanostructures of ZnO grown by various techniques and their application in DSSCs. The application of ZnO nanowires, nanorods in DSSCs became outstanding, providing a direct pathway to the anode for photo-generated electrons thereby suppressing carrier recombination. This is a novel characteristic which increases the efficiency of ZnO based dye-sensitized solar cells.

Keywords: semiconductor; nanostructures; Zinc Oxide; recombination; optoelectronics

1. Introduction

Nanophase ZnO can be synthesized into a variety of morphologies including nanowires, nanorods, tetrapods, nanobelts, nanoflowers, nanoparticles etc. Nanostructures can be obtained from various techniques such as vapour deposition or growth from solution, vapour-phase deposition (hydrothermal synthesis), chemical vapour deposition, metalorganic vapour phase epitaxy, electrodeposition, pulsed laser deposition, sputtering, sol-gel synthesis, spray pyrolysis, etc, at certain conditions, and also with the vapor-liquid-solid method. Rodlike nanostructures of ZnO can be produced via aqueous methods. They are attractive because of relatively low synthesis temperatures (<300°C) and absence of complex vacuum setup. The synthesis is typically carried out at temperatures of about 90°C, in an equimolar aqueous solution of zinc nitrate and hexamine, the later providing the basic environment. Certain additives, such as polyethylene glycol or polyethylenimine, can improve the aspect ratio (i.e., width-height ratio) of the ZnO nanowires (Baxter and Aydil 2005). Doping of the ZnO nanowires has been achieved by adding other metal nitrates to the growth solution. The morphology of the resulting nanostructures can be tuned by

*Corresponding author, Lecturer, E-mail: davidtyona@yahoo.com

^aProfessor, E-mail: uzosuji@yahoo.com ; rose.osuji@unn.edu.ng

^bSenior Lecturer, E-mail: fiezema@yahoo.com; fabian.ezema@unn.edu.ng

changing the parameters relating to the precursor composition (such as the zinc concentration and pH) or to the thermal treatment (such as the temperature and heating rate) (Baruah and Dutta 2009).

Aligned ZnO nanowires on pre-seeded silicon, glass and gallium nitride substrates have been grown in aqueous solutions using aqueous zinc salts such as Zinc nitrate and Zinc acetate in basic environments.

Pre-seeding substrates with ZnO creates sites for homogeneous nucleation of ZnO crystal during the synthesis. Common pre-seeding methods include in-situ thermal decomposition of zinc acetate crystallites, spincoating of ZnO nanoparticles and the use of various physical vapor deposition methods to deposit ZnO thin films. Pre-seeding can be performed in conjunction with top down patterning methods such as electron beam lithography and nanosphere lithography to designate nucleation sites prior to growth (Baruah and Dutta 2009). Aligned ZnO nanowires can be used in dye-sensitized solar cells and field emission devices.

Dye-sensitized solar cells (DSSCs) have the potential to convert solar power to electricity efficiently and at a low cost, making it promising solar cell architecture for large scale solar energy implementation. There are three main components to a DSSC; (1) a $\sim 10 \mu\text{m}$ thick film of wide band gap semiconductor nanoparticles such as TiO_2 or ZnO nanoparticles, (2) a monolayer of organic dye molecules absorbed onto the semiconductor, and (3) a liquid electrolyte containing the redox couple I^-/I_3^- which interpenetrates the dye-coated nanoparticles. When a photon excites the electron in the dye, it is injected into the semiconductor and is carried to the anode and through the load to the cathode where it reduces the I^- in the electrolyte. The I_3^- then regenerates the dye thus completing the circuit (Nakamura 2006, Nattestad *et al.* 2010).

In conventional nanoparticle DSSCs, the electrons diffuse to the anode by hopping 10^3 - 10^6 times between particles. With each hop, the electron can recombine with the electrolyte. The diffusion rate and recombination rate are both on the order of milliseconds, allowing recombination to limit the efficiency of the DSSC. However, ZnO nanowire DSSCs provide a direct path to the anode, which increases the diffusion rate without increasing the recombination rate and could therefore increase the efficiency of DSSCs (Nakamura 2006).

In the solution growth of ZnO nanowires, two types of crystal nucleation compete. Homogeneous nucleation produces undesired ZnO particles and heterogeneous nucleation produces nanowires. In the existing procedure, the homogeneous nucleation of ZnO particles dominates and depletes the precursor limiting the wire growth. To understand the kinetics and to hypothesize a mechanism that replicates the data, the rate of Zn^{2+} depletion was observed with time and various initial concentrations of reagents (Nakamura 2006, Gao *et al.* 2011).

2. Dye-sensitized solar cells

In the late 1960s it was discovered that illuminated organic dyes can generate electricity at oxide electrodes in electrochemical cells (Gerischer *et al.* 1968). In an effort to understand and simulate the primary processes in photosynthesis the phenomenon was studied at the University of Berkeley with chlorophyll extracted from spinach (bio-mimetic or bionic approach) (Tributsch and Calvin 1971). On the basis of such experiments electric power generation via the dye sensitization solar cell (DSSC) principle was demonstrated and discussed in 1972 (Tributsch 1972). The instability of the dye solar cell was identified as a main challenge. Its efficiency could, during the following two decades, be improved by optimizing the porosity of the electrode prepared from fine

oxide powder, but the instability remained a problem (Matsumura *et al.* 1980). A modern DSSC, is composed of a porous layer of titanium dioxide or Zinc oxide nanoparticles, covered with a molecular dye that absorbs sunlight, like the chlorophyll in green leaves. The dye-loaded titanium dioxide or Zinc oxide (semiconductor) is immersed under an electrolyte solution, above which is a platinum-based catalyst. As in a conventional alkaline battery, an anode (the semiconductor) and a cathode (the platinum) are placed on either side of a liquid conductor (the electrolyte) (Michael 2006).

Sunlight passes through the transparent electrode into the dye layer where it can excite electrons that then flow into the titanium dioxide. The electrons flow toward the transparent electrode where they are collected for powering a load. After flowing through the external circuit, they are re-introduced into the cell on a metal electrode on the back, flowing into the electrolyte. The electrolyte then transports the electrons back to the dye molecules (American Chemical Society 2006).

Dye-sensitized solar cells separate the two functions provided by silicon in a traditional cell design. Normally the silicon acts as both the source of photoelectrons, as well as providing the electric field to separate the charges and create a current (Gao *et al.* 2008). In the dye-sensitized solar cell, the bulk of the semiconductor is used solely for charge transport, the photoelectrons are provided from a separate photosensitivedye. Charge separation occurs at the surfaces between the dye, semiconductor and electrolyte (<http://lpi.epfl.ch/solarcellE.html> 1999).

The dye molecules are quite small (nanometer sized), so in order to capture a reasonable amount of the incoming light the layer of dye molecules needs to be made fairly thick, much thicker than the molecules themselves. To address this problem, a nanomaterial is used as a scaffold to hold large numbers of the dye molecules in a 3-D matrix, increasing the number of molecules for any given surface area of cell. In existing designs, this scaffolding is provided by the semiconductor material, which serves double-duty (Michael 2006).

3. Zinc oxide nanostructures for dye-sensitized solar cells

Zinc oxide nanostructures exist in a variety of morphologies including nanowires, nanorods, tetrapods, nanobelts, nanoflowers, nanoparticles etc. Nanostructures can be synthesised from various techniques including vapour deposition or growth from solution, vapour-phase deposition (hydrothermal synthesis), chemical vapour deposition, metalorganic vapour phase epitaxy, electrodeposition, pulsed laser deposition, sputtering, sol-gel synthesis, spray pyrolysis, etc, at certain conditions, and also with the vapor-liquid-solid method. This study will present a highlight of few nanostructures and growth techniques.

3.1 Zinc oxide nanowires

Dye-sensitized solar cells (DSSCs) based on a dye-sensitized wide-band-gap nanocrystalline semiconductor (typically TiO₂) film have attracted widespread attention as a potential, cost-effective alternative to silicon solar cells since they were first introduced by O'Regan and Grätzel in 1991. As one of the key components of dye-sensitized solar cells, the photoelectrode, composed of nanocrystalline semiconductor materials accumulated on a transparent conducting glass, has a very important influence on the photovoltaic performance (Nazeeruddin *et al.* 2001). It is well known that the energy conversion efficiency of DSSCs depends on the electron transport in the

photoelectrode. Therefore, one-dimensional structures such as rods or wires of semiconductor materials can greatly improve DSSCs efficiency by offering direct electrical pathways for photogenerated electrons, thus enhancing the electron transport in the photoelectrode. Recently, considerable efforts have been devoted to the synthesis of such 1D materials used as the photoelectrodes of DSSCs (Law *et al.* 2005, Kang *et al.* 2008, Jennings *et al.* 2008). Among various emerging 1D nanomaterials, ZnO, a wide-band-gap (3.37 eV) semiconductor with a large exciton binding energy of 60 meV at room temperature, is a promising alternative semiconductor to TiO₂. This is because the band gap and the energetic position of the valence band maximum and conduction band minimum of ZnO are very close to that of TiO₂ and that the wurtzite structure of ZnO favours the formation of ordered 1D structures, moreover, presenting better electron transport compared to TiO₂ (Law *et al.* 2005). Consequently, the solar cell using nanowire arrays as the photoelectrodes shows higher conversion efficiency compared to those using the disorderedly structured ZnO films (Law *et al.* 2005). In order to further improve the cell efficiency, the effective approaches currently applied are to control the morphology of ZnO nanostructure films, which can significantly increase dye loading and light harvesting (Gao *et al.* 2007) and to modify the surface of ZnO nanostructure films that can suppress carrier recombination (Law *et al.* 2005).

3.1.1 Growth of zinc oxide nanowires

Nakamura (2006) reported the solution growth of nanowires onto silicon substrates at a temperature of 35°C. The lengths of nanowires were measured and average nanowire lengths were determined as a function of time. Yang *et al.* (2009) carried out the synthesis of nanowires with high aspect ratio and different thicknesses of ZnO buffer layers by spin-coating method, dip-coating method and hydrothermal method. In their study, carrier recombination in ZnO nanowire-based dye-sensitized solar cells was effectively suppressed and the photovoltaic conversion efficiency enhanced by introducing the TiO₂ buffer layer prepared by sputtering method. They found that the different ZnO seed preparation methods strongly influenced the morphology and density of ZnO nanowire arrays, leading to the different performance of the DSSCs based on the ZnO nanowire films (Du *et al.* 2006). Fig. 1 shows the top-view and cross-section of Field-emission Scanning Electron Microscopy (FESEM) images of two samples prepared with 7.3 mM of Polyethyleneimine (PEI) for 30 hours on the Fluorine-doped tin oxide (FTO) substrates with ZnO seed layers prepared by spin-coating and dip-coating. The mean values of the nanowire dimension, the array density and aspect ratio were estimated from a statistical evaluation of FESEM images and are summarized in Table 1.

Table 1 Mean values of the nanowire dimensions, nanowire aspect ratio and array density for different ZnO seed preparation methods (Yang *et al.* 2009)

ZnO seed preparation Methods (nm)	Diameter (μm)	Length ratio	Nanowire aspect ($\times 10^9$ wires cm^{-2})	Density
Spin-coating				
Sample A1	200	9.5	48	2.1
Sample A2	195	9.1	47	2.2
Sample A3	210	8.2	39	2.0
Dip-coating				
Sample B1	120	9.5	79	1.5
Sample B2	150	8.2	55	1.6
Sample B3	130	9.8	75	1.2

Chao *et al.* (2010) reported the growth of ZnO nanowires in a furnace by chemical vapour deposition with gold as catalyst. Fig. 2 shows the tilt-view of the Scanning Electron Microscopy (SEM) image of ZnO nanowire arrays on the sapphire substrate. This image revealed that the ZnO wires are vertically aligned, the length of nanowire is around 1-2 μm and the diameter is in the range of 70-100 nm. The synthesis and characterization of three-dimensional heterogeneous grapheme nanostructures comprising continuous large-area graphene layers and ZnO nanostructures, fabricated via chemical vapor deposition, are reported by Lin *et al.* (2010). Electron microscopy investigation of the three-dimensional heterostructures shows that the morphology of ZnO nanostructures is highly dependent on the growth temperature. The morphology of the large-area graphene layers was identified via SEM as shown in Fig. 3(a),

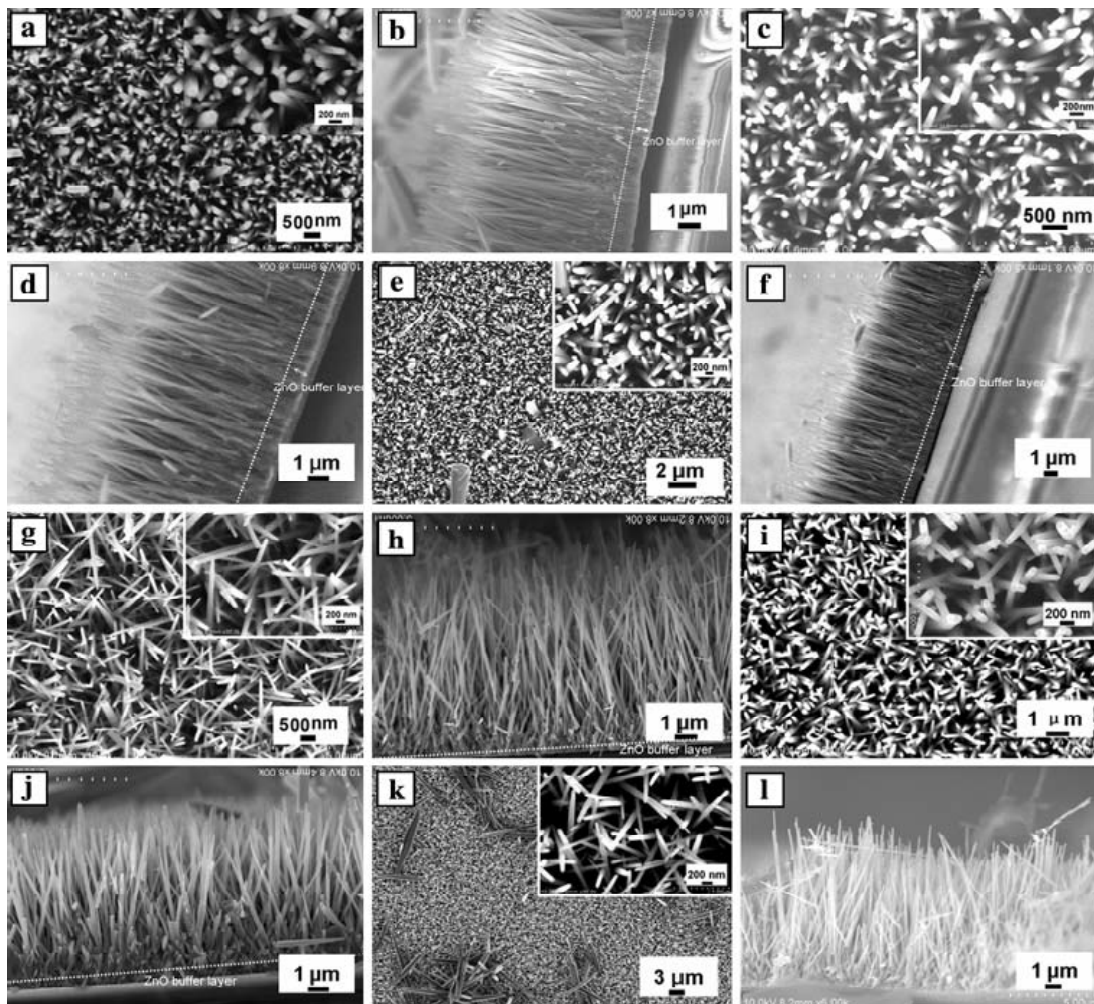


Fig. 1 SEM images of ZnO nanowire arrays grown on FTO substrates with different ZnO seed obtained from (a–f) the spin-coating method, (g–k) the dip-coating method. a, c, e, g, i and k correspond to top-view observations, b, d, f, h, j and l correspond to cross-sectional views. The insets show high magnification SEM images 1488 (Peng *et al.* 2011)

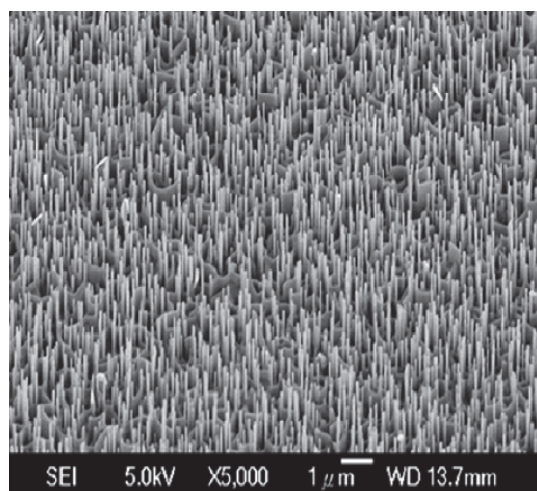


Fig. 2 Tilt-view SEM images of aligned ZnO nanowire arrays (Peng *et al.* 2011)

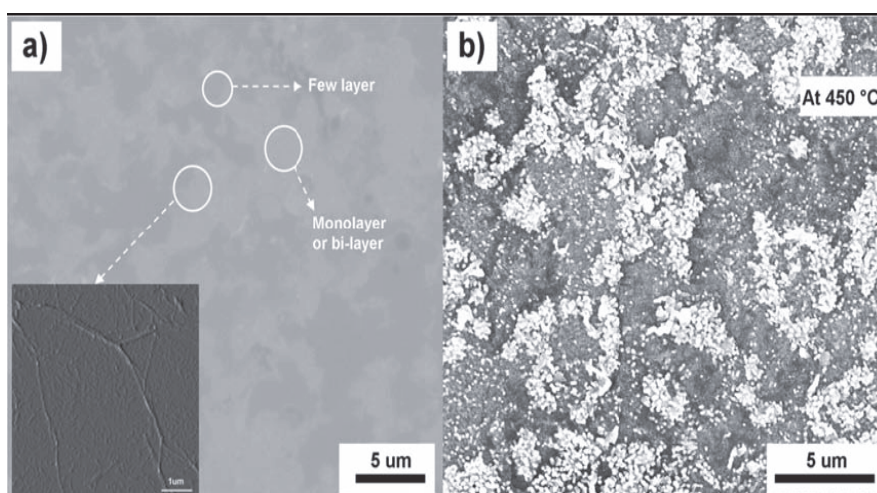


Fig. 3 (a) SEM image of a chemical vapor deposition-grown graphene layer on a SiO_2/Si substrate, (b) SEM image of ZnO nanostructures grown on the same chemical vapour deposition-graphene film at 450°C (Peng *et al.* 2011).

indicating regions of monolayers and few-layers. Boundary structures of graphene layers enhanced the growth of dense array of ZnO nanostructures, observed as bright regions shown in Fig. 3(b). The nanowires obtained by chemical and physical vapor deposition have generally good crystalline quality and important length (more often they are in nanobelt morphology) (Peng *et al.* 2011).

Fang *et al.* (2006) successfully synthesized aligned ZnO nanofibers in a dense array form and on a Zn substrate by hydrothermal treatment of Zn foil in an ammonia/alcohol/water mixed solution. Notably, the ZnO nanofibers are ultrathin (3-10 nm) with a length of ≈ 500 nm. It was reported that this was the first time that uniform, aligned, and ultrathin ZnO nanofibers have been obtained via a hydrothermal method in the absence of catalysts and at a relatively low temperature.

The photoluminescence measurements at room temperature revealed a significantly blue-shift near-band-edge emission at 373 nm (3.32 eV), which was ascribed to quantum confinement arising from the reduced size of the ultrathin ZnO nanofibers. Then, the hydrothermal synthesis of large-scale, ultralong ZnO nanowire and nanobelt arrays with honeycomb-like micropatterns has been realized by simple surface oxidation of zinc foil in aqueous solutions of NaOH and $(\text{NH}_4)_2\text{S}_2\text{O}_8$ at 150°C (Lu *et al.* 2006). This solution approach to fabricate 1D ZnO nanostructures with controlled morphologies and micropatterns can be easily scaled up and potentially extended to the fabrication and assembly of 1D nanostructures of other oxide systems. As shown in Fig. 4(a), a large scale thin film of long ZnO nanowire (20–50 mm) arrays formed unique micropatterns of honeycomb-like structures typically ranging from 10 to 30 mm in size on the Zn substrate after the Zn foil was immersed in the reaction solution containing 0.48 M NaOH and 0.095 M $(\text{NH}_4)_2\text{S}_2\text{O}_8$ and hydrothermally treated at 150°C for 2 days. An enlarged image of the honeycomb-like structure is shown in Fig. 4(b), which indicates that these structures were formed when the collapsing ZnO nanowires from opposite directions met to bundle together between two neighboring areas. The diameter of the ZnO nanowires is measured to range from 60 to 200 nm (Fig. 4(c)) and the electron diffraction (ED) pattern of a single nanowire suggests that each ZnO nanowire is a single crystal oriented along the c-axis (Fig. 4(d)), similar to the growth direction of the ZnO nanorods obtained at room temperature (Peng *et al.* 2011).

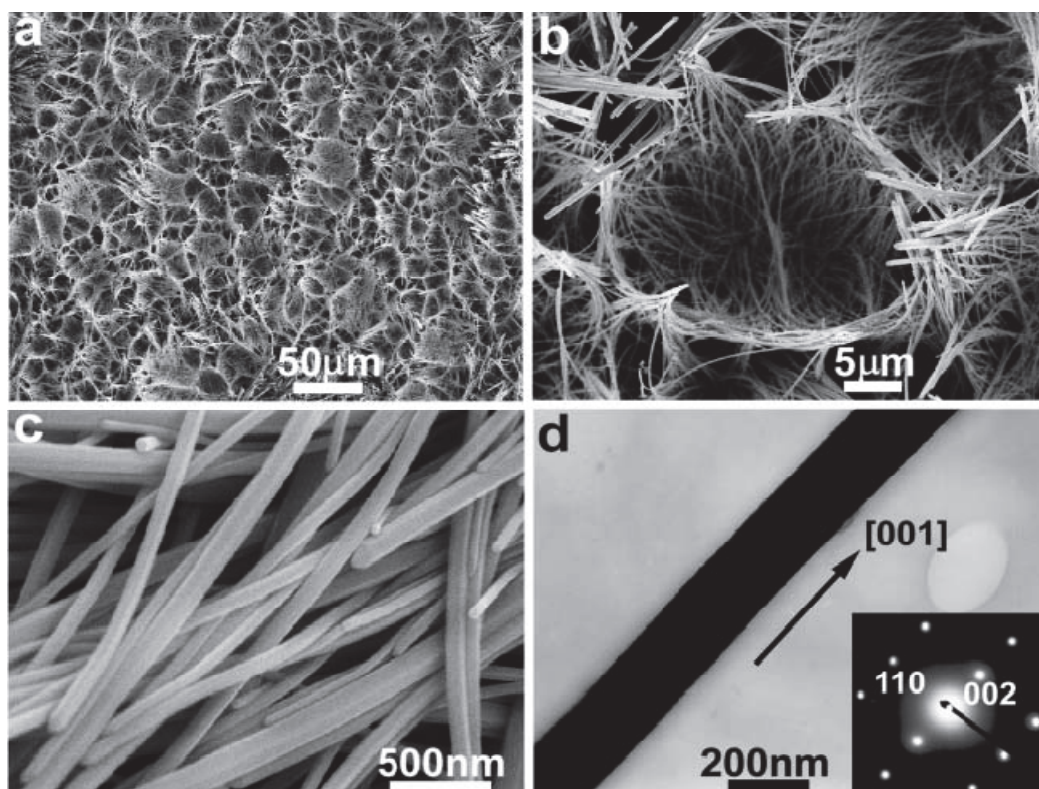


Fig. 4 SEM (a–c) and TEM (d) images of ZnO nanowire arrays hydrothermally grown on Zn foil at 150° C for 2 days (Peng *et al.* 2011)

Jason and Eraydemonstrated the growth of dense arrays of ZnO nanowires up to 8 microns long with 100 nm diameters by chemical bath deposition to investigate the effect of semiconductor morphology on DSSC performance, Fig. 5(a). Increasing nanowire length increases photocurrent and efficiency with no reduction in charge collection efficiency up to nanowire aspect ratios of at least 70, Fig. 5(b). Nanowire DSSCs show higher open circuit voltages than ZnO nanoparticle cells, indicating improved electron transport. Hybrid nanowire-nanoparticle cells exhibit even higher efficiencies by combining the increased light harvesting due to the nanoparticle surface area with faster transport through the nanowires. Furthermore, faster charge transport allows flexibility to choose other redox couples and solid state hole transport materials that will result in more efficient and robust DSSCs (Baxter and Aydil 2005).

3.2 Zinc oxide nanorods

One important limiting factor in the DSSC cell performance is electron transport. During its traversal to the photoelectrode, an electron is estimated to cross 103 to 106 nanoparticles (Brian and Michael 1991). The disorder structure of the nanoparticles film leads to enhanced scattering of free electrons, thus reducing electron mobility and causing electron recombination especially at the grain boundaries between the nanoparticles (Benkstein *et al.* 2003). The replacing of the nanoparticle film with an array of oriented single-crystalline nanorod offers the potential for improved electron transport leading to higher photoefficiencies. The pathways provided by the nanorods ensure the rapid collection of carriers generated throughout the device as the nanorod provide a direct path from the point of photogeneration to the conducting substrate. This greatly reduces the electron recombination losses of the photogenerated charge-carriers due to the fewer grain boundaries in charge transportation process. Moreover, electron transport in the crystalline rod is expected to be several orders of magnitude faster than percolation through a random polycrystalline network (Michael 2000).

3.2.1 Growth of zinc oxide nanorods

Patcharee and Susumu, 2006 chemically synthesized an array of ZnO nanorods on FTO substrate. A procedure which involves two steps; zinc acetate solution was dropped onto substrates

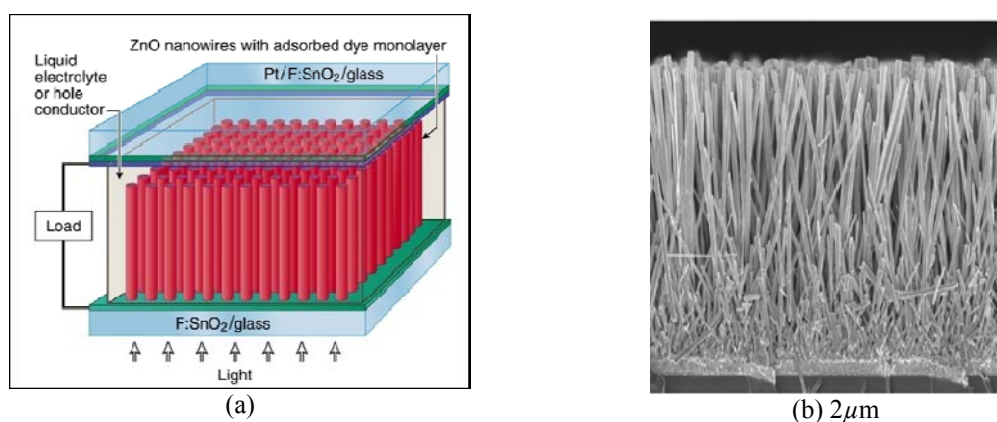


Fig. 5 (a) Schematic of ZnO nanowire dye sensitized solar cell (b) cross-sectional SEM image of ZnO nanowire array (Baxter and Aydil 2005)

by spin coating, and then the substrates were dried and annealed in order to form the nanocrystal seeds on the substrates. Secondly, vertical ZnO nanorod arrays from the nanocrystal seeds were grown by immersing the seeded substrates in precursor solution containing $\text{Zn}(\text{NO}_3)_2$ and 0.80 M NaOH at 110°C with different growth time intervals.

The crystalline structure of the samples was evaluated by X-ray diffraction (XRD, RIGAKU RINT 2100) and the microstructure of the prepared materials analyzed by scanning electron microscopy (SEM, JEOL JSM-6500FE). The dye-sensitized solar cell was prepared for photovoltaic measurement by soaking the ZnO electrodes in 0.3 mM of ruthenium (II) dye (known as N719, Solaronix) in a *t*-butanol/acetonitrile (1:1, in vol%) solution. The electrodes were washed with acetonitrile, dried, and immediately used for measuring photovoltaic properties. The electrolyte was composed of 0.6 M dimethylpropylimidazolium iodide, 0.1 M lithium iodide (LiI), 0.05 M iodide (I₂), and 0.5 M 4-*tert*-butylpyridine in acetonitrile.

Fig. 6 shows typical SEM images of the ZnO nanorods arrays grown on FTO substrate by this method. The low-magnification images (A, C) show a well-aligned high-density ZnO nanorods growing uniformly in large area on the substrate. From the high magnification image (D), it can be seen that high-density ZnO nanorods with well-defined hexagonal facets were grown vertically on the substrate. The cross-sectional view (B) of nanorods arrays demonstrated that the ZnO grew vertically from the substrate. A typical XRD pattern is shown in Fig. 7, the intensity of the peak assigned to the (002) plane of wurtzite ZnO was markedly strong and the diffraction peaks of other crystal planes disappeared or very weak revealing that ZnO nanorods were formed through elongation along the *c*-axis perpendicularly to the substrate.

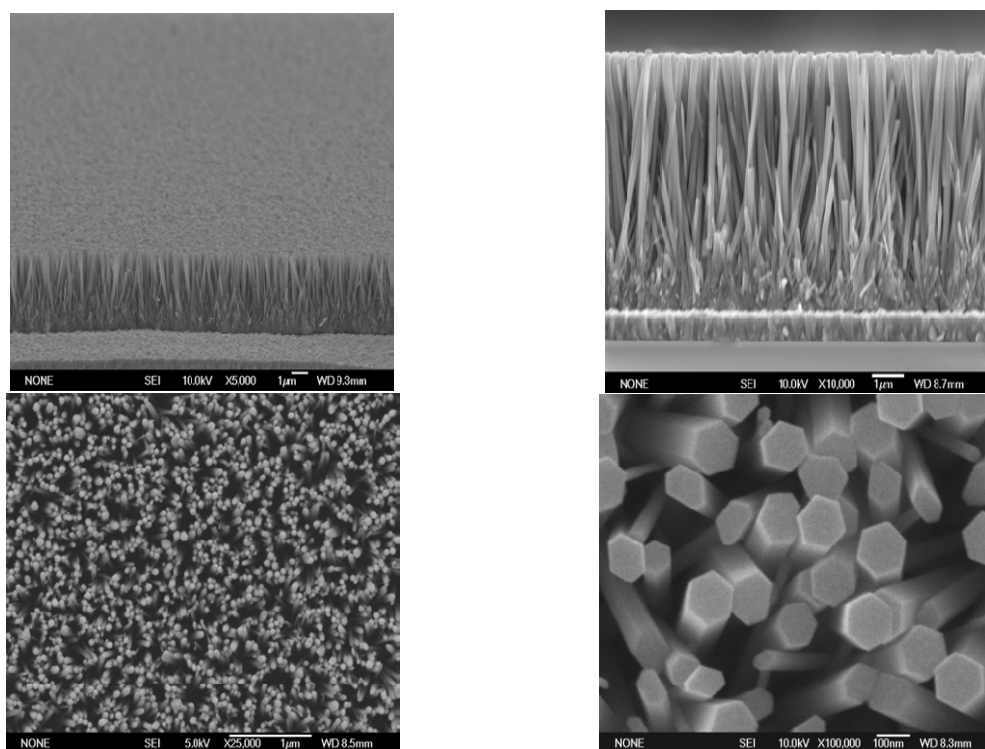


Fig. 6 SEM images of ZnO nanorods grown on FTO substrate (A) tilt view, (B) side view, (C) top view at low magnification, and (D) top view at high magnification (Charoensirithavorn and Yoshikawa 2006)

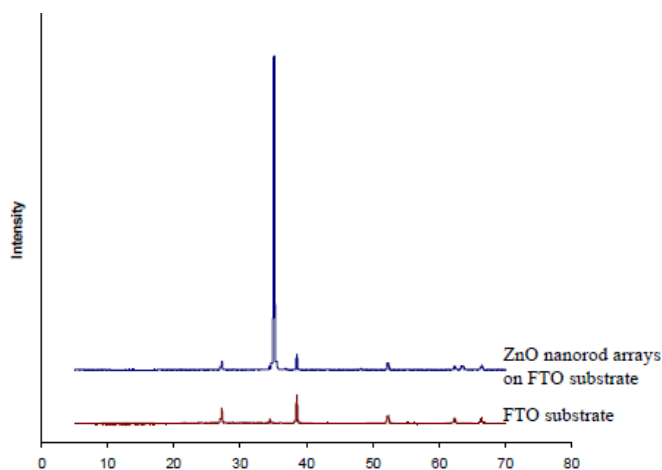


Fig. 7 XRD patterns of FTO substrate and ZnO nanorod arrays on FTO (Charoensirithavorn and Yoshikawa 2006)

Currently, work has been carried out on nanorod arrays grown on an FTO glass substrate but there is a disadvantage to this structure - the photoelectrode and the Transparent Conducting Oxide (TCO) layer are made of different materials and a heterogeneous interface exists between them. This interface forms a source for electron scattering. Chen *et al.* recently demonstrated a novel DSSC design, growing ZnO nanorods on the top of a ZnO film. The ZnO film replaces the FTO layer as the TCO layer. ZnO is a good TCO material because it has an energy gap of $E_g = 3.4$ eV, hence, is transparent in the visible spectral range. Their structure was grown by a two-step process: a Ga-doped ZnO film was first grown on a substrate, after which ZnO nanorods were grown on top of the film. This structure eliminated the heterojunction between the TCO film and the nanorods. A power conversion efficiency of 0.77% was achieved by Chen *et al.* (Lai *et al.* 2011). A similar work was reported by Tubtimtae *et al.* in which indium-doped ZnO was used as a seed substrate for the growth of ZnO nanorods (Tubtimtae *et al.* 2012).

In an earlier work carried out by Lai *et al.*, they fabricated Chen's new-structure DSSCs using a method simpler than Chen's method. Lai, used a one-step method to grow ZnO nanorods and a ZnO film. A power conversion efficiency of 0.73% was achieved. In a recent work they improved on the one-step growth and fabrication of the solar cells. Investigation of the photovoltaic properties of the ZnO-nanorod DSSCs showed the new DSSCs to yield efficiencies much higher than those of Chen's and their earlier new-structure ZnO-nanorod DSSCs. There are two notable features in the new DSSC structure: (1) the junction between the TCO film and the nanorods is completely eliminated; (2) the TCO and the photoelectrode are made of the same material, hence, electron conduction and power conversion efficiency are expected to improve (Kang *et al.* 2008).

In their recent work (i.e., Lai *et al.*), ZnO nanorods and a ZnO film were cogrown by a one-step catalyst-free chemical-vapor-deposition (CVD) method. Single-crystalline c-plane (0001) sapphire substrates were loaded into an alumina boat, which was then placed inside a one-inch quartz tube in a horizontal tube furnace. The substrate was placed 7-11 cm downstream from the Zn source material. The furnace was heated to 870°C at a heating rate of 12°C/min and then maintained at the heated temperature for 40 min. Ar and O₂ gases were fed into the quartz tube at flow rates of 16.4

sccm (Ar) and 1.8 sccm (O₂). During the first growth stage, a ZnO film grew on the substrate. In the second growth stage, ZnO nanorods were grown on top of the ZnO film. The DSSCs were fabricated by immersing the ZnO nanorods in a 60°C, 0.5 mM D149 dye (Mitsubishi paper) solution (a mixture of 1mM chenodeoxycholic acid in tert-butyl alcohol and acetonitrile, 1:1 volume ratio) for 8h. They also investigated the performance of the cells sensitized with the commonly used dye-N719 (0.3 mM). An FTO glass with a 150 μm-thick Pt foil attached to it was used as the counter-electrode. The photoanode and the counter-electrode were assembled into a solar cell using a 25μm-thick surlyn spacer. The electrolyte was composed of 0.5M LiI, 0.05M I₂, 0.5M 4-tert-butylpyridine, and 0.6M butylmethylimidazolium iodide in acetonitrile and valeronitrile. The electrolyte was injected into the cell through two predrilled holes (size 1 mm) on the counterelectrode. The active area of the cell, limited by the size of the grown sample, was ~ 2 mm×2 mm Lai *et al.* (2011).

Fig. 8(a) shows a field-emission scanning electron microscopic (FESEM) cross-sectional image of the ZnO nanorods grown by the one-step CVD process. The nanorods have diameters in the range of 150 - 220 nm and lengths of ~ 12 μm. A layer of ZnO film (thickness ~ 2.5 μm) can be clearly seen in the picture. The diameter and film thickness of the nanorods are found to decrease as the O₂ flow rate was increased. The nanorods are roughly perpendicular (angle 60°-90°) to the ZnO film. Figs. 8(b) and (c) show a TEM image of a single nanorod and its electron diffraction pattern, which reveals the single-crystalline nature of the nanorod (Lai *et al.* 2011).

The X-ray diffraction pattern, shown in figure 9, reveals that the nanorods are of the wurtzite structure with lattice constants of $a = 3.176 \text{ \AA}$, $c = 5.187 \text{ \AA}$.

3.3 ZnO nanotubes

Nanotubes differ from nanowires in that they typically have a hollow cavity structure. An array of nanotubes possesses high porosity and may offer a larger surface area than that of nanowires.

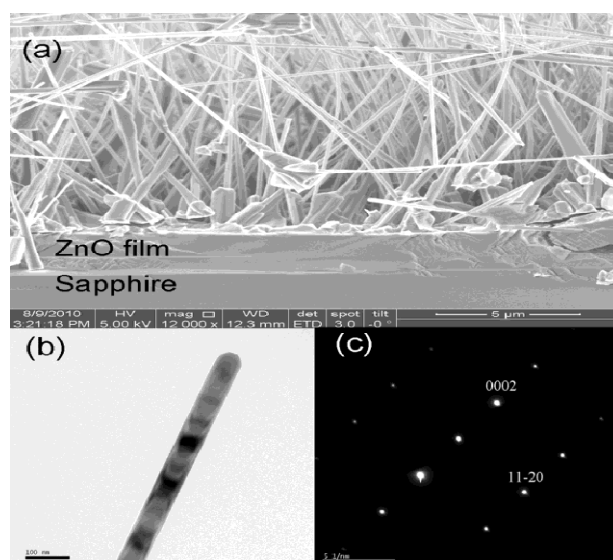


Fig. 8 (a) FESEM image of ZnO nanorods on top of a ZnO film, (b) TEM image of a single ZnO nanorod, (c) Electron diffraction pattern of a single nanorod (Lai *et al.* 2011)

The synthesis of ZnO nanotube arrays can be achieved by using a modified method for the aqueous growth of ZnO nanowires at low temperatures. An overall conversion efficiency of 2.3% has been reported for DSSCs with ZnO nanotube arrays possessing a nanotube diameter of 500nm and a density of 5.4×10^6 per square centimeter. ZnO nanotube arrays can also be prepared by coating anodic aluminum oxide (AAO) membranes via atomic layer deposition (ALD). However, it yields a relatively low conversion efficiency of 1.6%, primarily due to the modest roughness factor of commercial membranes (Zhang *et al.* 2009).

3.4 ZnO nanotips

By using Metalorganic Chemical Vapor Deposition (MOCVD) processing methods, ZnO nanotip arrays with different lengths can be synthesized. The DSSC performance of these nanotips has been investigated in previous studies (Chen *et al.* 2008). The results confirmed that the energy-conversion efficiency of the cells increased with the length of the ZnO nanotips due to the increase in surface area of the photoelectrode film. An overall conversion efficiency of 0.55% was obtained for 3.2-mm-long ZnO nanotips. It has been reported that ZnO nanotips present a maximum overall conversion efficiency at higher light intensities than in the case of TiO₂ nanoparticles. This implies a nontrap-limited electron transport in the respect that the nanotips provide a faster conduction pathway for electron transport. This feature allows for the use of ZnO nanotips in the fabrication of more stable and efficient DSSCs under high illumination. It has also been demonstrated that the overall conversion efficiency could be increased to 0.77% by combining the ZnO nanotips with a Ga-doped ZnO film as a transparent conducting layer (Zhang *et al.* 2009).

4. Other nanostructured ZnO films

ZnO nanostructures with other morphologies, such as nanosheets, nanobelts, and nanotetrapods, have also been studied for DSC applications on account of the fact that they also have a large specific surface area. However, for these nanostructures, the specific surface area is not the only factor that determines the photovoltaic efficiency of the DSC. Solar-cell performance

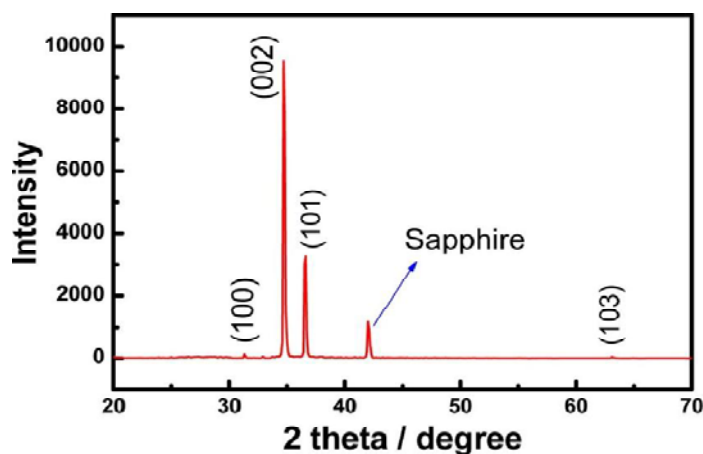


Fig. 9 X-ray diffraction pattern of the ZnO nanorods (Lai *et al.* 2011)

is also believed to be significantly affected by the geometrical structure of the photoelectrode films, which provides particular properties in terms of the electron transport and/or light propagation (Zhang *et al.* 2009).

4.1 Nanosheets

ZnO nanosheets are quasi-two-dimensional structures that can be fabricated by a rehydrothermal growth process of previously hydrothermally grown ZnO nanoparticles (Suliman *et al.* 2007). A film with dispersed ZnO nanosheets (Fig. 10(a)) used in a DSC has been shown to possess a relatively low conversion efficiency, 1.55%, possibly due to an insufficient internal surface area. It seems that ZnO nanosheet-spheres (Fig. 10(b)) prepared by hydrothermal treatment using oxalic acid as the capping agent may have a significant enhancement in internal surface area, resulting in a conversion efficiency of up to 2.61% (Akhtar *et al.* 2008). As for nanosheet-spheres, the performance of the solar cell is also believed to benefit from a high degree of crystallinity and, therefore, low resistance with regards to electron transport (Zhang *et al.* 2009).

4.2 Nanobelts

Zhang *et al.* (2009) prepared ZnO films with nanobelt arrays through an electrodeposition method for DSC applications. In fabricating these nanobelts, polyoxyethylene cetyether was added in the electrolyte as a surfactant (i.e., an agent that reduces the surface tension of liquids so that the liquid spread out rather than collecting in droplets). The ZnO nanobelt array obtained shows a highly porous stripe structure (Fig. 10(c)) with a nanobelt thickness of 5 nm, a typical surface area of $70 \text{ m}^2 \text{ g}^{-1}$, and a photovoltaic efficiency as high as 2.6%.

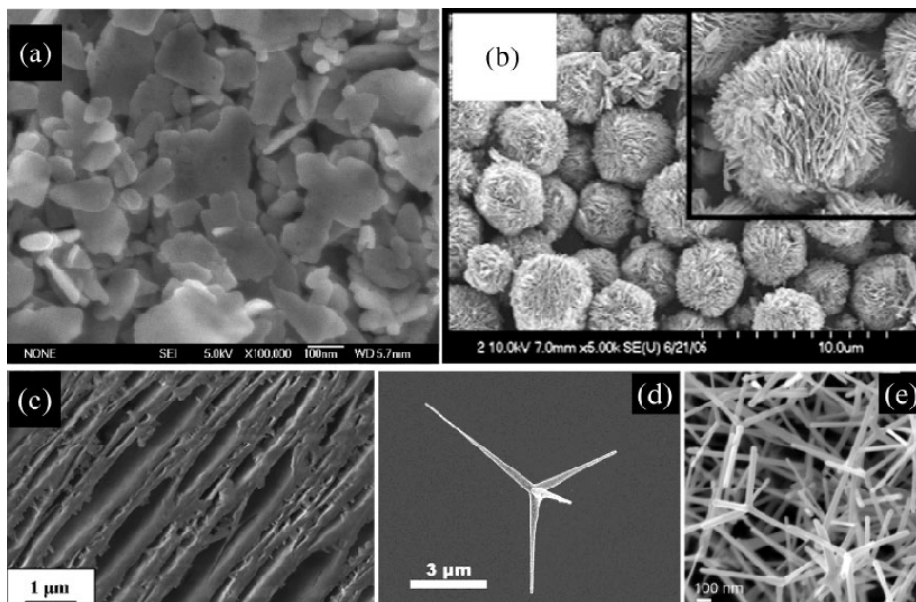


Fig. 10 SEM images of nanostructured ZnO films: (a) dispersed nanosheets, (b) nanosheet-assembled spheres, (c) nanobelt array, (d) a ZnO tetrapod formed in a three-dimensional structure with four arms extending from a common core, (e) networked film with interconnected ZnO tetrapods (Zhang *et al.* 2009)

4.3 Tetrapods

A ZnO tetrapod possesses a three-dimensional structure consisting of four arms extending from a common core (Fig. 10(d)). The length of the arms can be adjusted within the range of 1-20 nm, while the diameter can be tuned from 100nm to 2 nm by changing the substrate temperature and oxygen partial pressure during vapor deposition. Multiple-layer deposition can result in tetrapods connected to each other so as to form a porous network with a large specific surface area (Fig. 10(e)). The films with ZnO tetrapods used in DSCs have achieved overall conversion efficiencies of 1.20-3.27%. It was reported that the internal surface area of tetrapod films could be further increased by incorporating ZnO nanoparticles with these films, leading to significant improvement in the solar-cell performance (Zhang *et al.* 2009).

5. Conclusions

In summary, the work presents a review of different ZnO nanostructures for DSSCs under different growth methods (seed preparation methods) and their effects in DSSCs. The nanostructures considered here include nanowires, nanorods, nanotubes, nanotips etc. Among various emerging 1D nanomaterials, ZnO, a wide-band-gap (3.37 eV) semiconductor with a large exciton binding energy of 60 meV at room temperature, is a promising alternative semiconductor to TiO₂ in DSSCs technology. It has been revealed that ZnO nanostructures now serve as effective photoelectrode materials for DSSCs to provide direct electrical pathway for photo-generated electrons. Also, Yang *et al* was able to show that the different ZnO seed preparation methods can strongly influence the morphology and density of ZnO nanostructures. Encouraging progress in the research of nanostructured ZnO materials is being daily accomplished as reviewed in this article.

References

- Akhtar, M.S., Khan, M.A., Jeon, M.S. and Yang, O.B. (2008), "Controlled synthesis of various ZnO nanostructured materials", *Electrochim. Acta*, **53**, 7869.
- American Chemical Society (ACS) (2006), "Ulthathin, Dye-sensitized Solar Cells Called Most Efficient To Date", Science Daily.
- Baruah, S. and Dutta, J. (2009), "Hydrothermal growth of ZnO nanostructures", *Sci. Technol. Adv. Mater.*, **10**, 013001.
- Baxter, J.B. and Aydil, E.S. (2005), "Nanowire-based dye-sensitized solar cells", *Applied Physics Letters*, **86**, 053114.
- Benkstein, K.D., Kopidakis, N., Lagemaat, J.V. and Frank, A.J. (2003), "Influence of the percolation network geometry on electron transport in dye-sensitized titanium dioxide solar cells", *J. of Physical Chem. B.*, **107**(31), 7759-7767.
- Brian, O.R. and Michael, G. (1991), "A low-cost, high-efficiency solar-cell based on dye sensitized colloidal TiO₂ films", *Nature*, **353**, 737-740.
- Chao, H.Y., Cheng, J.H., Lu, J.Y., Chang, Y.H., Cheng, C.L. and Chen, Y.F. (2010), "Growth and characterization of type-II ZnO/ZnTe core-shell nanowire arrays for solar cell applications", *Superlattices and Microstructures*, **47**(1), 160-164.
- Charoensirithavorn, P. and Yoshikawa, S. (2006), "Dye-sensitized solar cell based on ZnO nanorod arrays",

- Sustainable Energy and Environment*, B-024(O).
- Chen, H.H., Du Pasquier, A., Saraf, G., Zhong, J. and Lu, Y. (2008), "Dye-sensitized solar cells using ZnO nanotips and Ga-Doped ZnO", *Semicond. Sci. Technol.*, **23**, 045004.
- Du Pasquier, A., Chen, H.H. and Lu, Y.C. (2006), "Dye-sensitized solar cells using well- aligned Zinc Oxide nanotip arrays", *Appl. Phys. Lett.*, **89**, 253513.
- Dye-Sensitized Solar Cells, <http://lpi.epfl.ch/solarcellE.html>, 2 February, 1999. Retrieved 13 January, 2012.
- Fang, Y., Pang, Q., Wen, X., Wang, J. and Yang, S. (2006), "Synthesis of ultrathin ZnO nanofibers aligned on a Zinc substrate", *Small.*, **2**(5), 612-615.
- Gao, F., Wang, Y., Zhang, J., Shi, D., Wang, M., Humphry-Baker, R., Wang, P., Zakeeruddin, S.M. and Grätzel, M. (2008), "A new heteroleptic ruthenium sensitizer enhances the absorptivity of mesoporous titania film for a high efficiency dye-sensitized solar cell", *Chemical Communications*, **23**, 2635.
- Gao, X. D., Li, X.M., Yu, W.D., Qiu, J.J. and Gan, X.Y. (2007), "Preparation of nanoporous TiO₂ thick film and its photoelectrochemical properties sensitized by Merbromin", *J. Inorg. Mat.*, **22**(6), 1079-1085.
- Gao, X., Wang, C., Gan, X. and Li, X. (2011), "Ordered semiconductor photoanode films for dye-sensitized solar cells based on Zinc Oxide-Titanium Oxide hybrid nanostructures", Institute of Ceramics, P.R. China.
- Gerischer, H., Michel-Beyerle M., Rebentrost, E. and Tributsch, H. (1968), "Sensitization of charge-injection into semiconductors with large band gap", *Electrochim. Acta*, **13**, 1509-1515.
- Grätzel, M. (2008), "A new heteroleptic ruthenium sensitizer enhances the absorptivity of mesoporous titania film for a high efficiency dye-sensitized solar cell", *Chemical Communications*, **23**, 2635-7.
- Jennings, J.R., Ghicov, A., Peter, L.M., Schmuki, P. and Walker, A.B. (2008), "Dye-sensitized solar cells based on oriented TiO₂ nanotube array: transport, trapping and transfer electrons", *J. Am. Chem. Soc.*, **130**, 13364.
- Kang, S.H., Choi, S.H., Kang, M.S., Kim, J.Y., Kim, H.S., Hyeon, T. and Sung, Y.E. (2008), "Nanorod-based dye-sensitized solar cells with improved charge collection efficiency", *Adv. Mater.*, **20**(1), 54-58.
- Lai, M.H., Lee, M.W., Wang, G. and Tai, M.F. (2011), "Photovoltaic performance of new- structure ZnO-nanorod dye-sensitized solar cells", *Int. J. Electrochem. Sci.*, **6**, 2122-2130.
- Law, M., Greene, L.E., Johnson, J.C., Saykally, R. and Yang, P. (2005), "Nanowire dyesensitized solar cells", *Nature Materials.*, **4**(6), 455-459.
- Li, Q.C., Kumar, V., Li, Y., Zhang, H.T., Marks, T.J. and Chang, R.P.H. (2005), "Fabrication of ZnO nanorods and nanotubes in aqueous solutions", *Chem. Mater.*, **17**, 1001.
- Lin, J., Penchev, M., Wang, G., Paul, R.K., Zhong, J., Jing, X., Ozkan, M. and Ozkan, C.S. (2010), "Heterogeneous graphene nanostructures: ZnO nanostructures grown on large-area graphene layers", *Small.*, **6**(21), 2448-2452.
- Lu, C., Qi, L., Yang, J., Tang, L., Zhang, D. and Ma, J. (2006), "Hydrothermal growth of largescale micropatterned arrays of ultralong ZnO nanowires and nanobelts on zinc substrate", *Chemical Communications*, **42**(33), 3551-3553.
- Matsumura, M., Matsudaira, S., Tsubomura, H., Takata, M. and Yanagida, H. (1980), "Dye sensitization and surface structures of semiconductor electrodes", *Ind. Eng. Chem. Prod. Res. Dev.*, **19**(3), 415-421.
- Michael, B. (2006), "Nanowires could lead to improved solar cells", Newswire Today.
- Michael, G. (2000), "Perspectives for dye-sensitized nanocrystalline solar cells", *Progress in Photovoltaics: Research and Applications*, **8**(1), 27-38.
- Nakamura, Y. (2006), "Solution-growth of Zinc Oxide nanowires for dye-sensitized solar cells", NNIN REU 2006 Research Accomplishments, 74.
- Nattestad, A., Mozer, A.J., Fischer, M.K., Cheng, Y.B., Mishra, A., Bäuerle, P. and Bach, U. (2010), "Highly efficient photocathodes for dye-sensitized tandem solar cells", *Nature Materials*, **9**(1), 31-5.
- Nazeeruddin, M.K., Pechy, P., Renouard, T., Zakeeruddin, S.M., Humphry-Baker, R., Comte, P., Liska, P., Cevey, L., Costa, E., Shklover, V., Spiccia, L., Deacon, G.B., Bignozzi, C.A. and Grätzel, J. (2001), "Engineering of efficiency panchromatic sensitizers for nanocrystalline TiO₂-based solar cells", *Am. Chem. Soc.*, **123**, 1613.
- O'Regan, B. and Grätzel, M. (1991), "A low-cost high-efficiency solar cell based on dye-sensitized colloidal

- TiO₂ films”, *Nature*, **353**(6346), 737-740.
- Peng, Q. and Qin, Y. (2011), “ZnO nanowires and their application for solar cells”, Nanchang, 330063 China.
- Suliman, A.E., Tang, Y.W. and Xu, L. (2007), “Preparation of ZnO nanoparticles and nanosheets and their application to dye-sensitized solar cells”, *Sol. Energ. Mat. Sc.*, **91**, 1658.
- Tributsch, H. and Calvin, M. (1971), “Electrochemistry of excited molecules: photoelectrochemical reactions of chlorophylls”, *Photochem. Photobiol.* **14**, 95-112.
- Tributsch, H. (1972), “Reaction of excited chlorophyll molecules at electrodes and in photosynthesis”, *Photochem. Photobiol.*, **16**, 261-269.
- Tubtimtae, A. and Lee, M. (2012), “ZnO nanorods on undoped and indium-doped ZnO thin films as a TCO layer on nonconductive glass for dye-sensitized solar cells”, *Superlattices and Microstructures*, **52**(5), 987-996.
- Yang, W., Wan, F., Chen, S. and Jiang, C. (2009), “Hydrothermal growth and application of ZnO nanowire films with ZnO and TiO₂ buffer layers in dye-sensitized solar cells”, *Nanoscale Res Lett.*, **4**, 1486-1492.
- Zhang, Q., Dandeneau, C.S., Zhou, X. and Cao, G. (2009), “ZnO nanostructures for dye-sensitized solar cells”, *Adv. Mater.*, **21**, 4087-4108.

CC